

Learning Neural Differential Algebraic Equations via Operator Splitting

James Koch¹, Madelyn Shapiro¹, Himanshu Sharma¹, Draguna Vrabie¹, Ján Drgoňa^{1,2}

Abstract—Differential-Algebraic Equations (DAEs) describe the temporal evolution of systems that obey both differential and algebraic constraints. Of particular interest are systems that contain implicit relationships between their components, such as conservation relationships. Here, we present an Operator Splitting (OS) numerical integration scheme for learning unknown components of Differential-Algebraic Equations from time-series data. This methodology is built upon the concept of the Universal Differential Equation; that is, a model constructed as a system of Neural Ordinary Differential Equations informed by theory from particular science domains. In this work, we show that the proposed OS-based time-stepping scheme is suitable for relevant system-theoretic data-driven modeling tasks. Presented examples include (i) the inverse problem of tank-manifold dynamics and (ii) discrepancy modeling of a network of pumps, tanks, and pipes. Our experiments demonstrate the proposed method’s robustness to noise and extrapolation ability to (i) learn the behaviors of the system components and their interaction physics and (ii) disambiguate between data trends and mechanistic relationships contained in the system.

I. INTRODUCTION

Modeling and simulation of systems via Differential-Algebraic Equations (DAEs) can be difficult, both in terms of formulation as well as numerical implementation. Common issues include (i) over- or under-constraining states and (ii) incorrect model specification, either of which can lead to a prohibitively challenging modeling task [1]. While many such algebraic relationships may be known (e.g., mass is conserved through a pipe), incorporating these algebraic relationships into well-established data-driven modeling paradigms is non-trivial. Here, measurement noise, partial observations, and missing or incorrect physics confound the ability to effectively build data-driven models that obey algebraic constraints. In practice, simplified models can be adopted that capture improperly specified or missing physics at a given fidelity. A common approach is to employ a closure model [2], i.e., a surrogate for the full-fidelity physics inserted into a lower-fidelity model. Closure models have enabled major advancements in scientific computing but still traditionally rely upon rigorous reduction from first principles physics to derive required simplified relationships [3].

A. Contributions

To address this issue, we present a novel framework for the data-driven modeling of DAEs. Our framework integrates ideas from neural timesteppers [4], operator splitting methods [5], and Physics-Informed Neural Networks (PINNs) [6]

to accommodate algebraic relationships in the context of neural ordinary differential equations (NODEs) [7]. We demonstrate the utility of these methods on two data-driven closure modeling tasks: (i) a tank-manifold problem, where one needs to ‘invert’ the model to provide an estimate of a property of a model component, and (ii) a tank-pipe-pump network for learning unknown nonlinear interactions. Our specific contributions are:

- Taking inspiration from the well-established field of operator splitting, we extend neural timesteppers to appropriately integrate DAEs.
- We accomplish this via an algebra surrogate layer that modifies algebraic states of a system, while an ODE Solver integrates differential states.
- We demonstrate the utility of the method in data-driven parameter estimation problems such as canonical closure and inverse modeling of constrained networked system dynamics.
- We open-source the implementation of the proposed method¹ to promote reproducibility and adoption.

The paper is organized as follows. Section II provides a brief background. Section III defines the problem of interest. Section IV details our proposed methodology and its implementation. Example results are provided in Section V, followed by a discussion in Section VI.

B. Related Work

1) *Machine Learning for Dynamical Systems*: Methods for learning dynamics from data exist on a continuum from ‘black-box’ models to ‘white-box’ models [8]. The ‘black-box’ modeling task is performed without regard to the underlying system or domain knowledge and includes Recurrent Neural Networks (RNNs) and their variants (e.g., LSTMs) [9], neural state space models [10], [11], neural timesteppers [4], sparse symbolic regression [12], and Neural ODEs (NODEs) [7], [13], [14]. Often, such models extract salient features in the training data to infer future states. However, satisfying algebraic constraints in these data-driven models is not trivial. ‘White-box’ models use domain knowledge to constrain models to match expected dynamics, often leading to parameter-tuning problems [15]. In ‘gray-box’ models, recently referred to as physics-informed machine learning [16], prior knowledge is incorporated in a manner to constrain a ‘black-box model’. Neural ODEs constructed with domain knowledge, termed *Universal Differential Equations* [17], [18], are an attractive modeling platform for these problems because of their flexibility in encoding structural priors.

¹Pacific Northwest National Laboratory,

²Department of Civil and Systems Engineering, and the Ralph O’Connor Sustainable Energy Institute, Johns Hopkins University, jdrgono1@jh.edu

¹<https://github.com/pnnl/NeuralDAEs>

2) *Data-driven Modeling of DAEs*: If the DAE is well-characterized, the parameter estimation, inverse design, and control tasks are possible through an adjoint sensitivity analysis [19], [20], [21]. This strategy is generally successful if (i) the index of the underlying DAE is low and (ii) all constituent physics are known. Recent works have begun to address some common issues regarding data-driven DAE-based models. Moya and Lin [22] use explicit Runge-Kutta time-stepping to combine semi-explicit DAEs into machine learning frameworks, which they demonstrate by modeling power networks. Xiao et al. [23] construct neural ODE and DAE modules to forecast a regional power network. Huang et al. [24] adopt a simplified approach to the construction of a surrogate system for sequence-to-sequence mappings for DAEs. These studies share features of expressing the learning task in terms of a semi-explicit DAE with varying degrees of parameterization and integration of domain knowledge. In addition to these studies, Zhong et al. [25] addressed contact modeling in multi-body dynamics, the authors in the work handled a constraint update architecture with similar explicit time-stepping as in Moya [22] and Xiao [23].

While the specific treatment of each of these domain-focused problems varies, each leverages a form of a multi-step integration technique that separates the evolution of differential and algebraic states. We recognize that the commonality of these works holds the potential for a generalization of standard NODE integration. Specifically, we recast these ideas under operator splitting methods, where integration is split into simpler, sequential sub-tasks. In effect, we propose a new class of neural timesteppers suitable for the data-driven modeling of DAEs with partially unknown dynamics.

II. BACKGROUND

A. Differential-Algebraic Equations

Differential-Algebraic Equations (DAEs) are systems comprising differential and algebraic relationships that describe the evolution of a system's states. Specifically, we are concerned with semi-explicit DAEs written as:

$$\begin{aligned} \frac{dx}{dt} &= f(x, y, u), \\ 0 &= g(x, y, u), \end{aligned} \quad (1)$$

where $x \in \mathbb{R}^{n_x}$ are the differential states of a system that evolve according to the vector field defined by $f: \mathbb{R}^{n_x} \times \mathbb{R}^{n_y} \times \mathbb{R}^{n_u} \rightarrow \mathbb{R}^{n_x}$, $y \in \mathbb{R}^{n_y}$ are the algebraic states, and $u \in \mathbb{R}^{n_u}$ are exogenous inputs. The algebraic states y evolve such that the algebraic relationships, defined by $g(x, y, u) = 0$, are satisfied for all time t .

A standard DAE solution approach is to transform the system into a set of ODEs to be integrated with standard numerical solvers. This process is termed *index reduction* [1]. The index of a DAE is a distance measure between a DAE and its associated ODE: an index-1 DAE requires one differentiation of algebraic relationships to yield a consistent set of ODEs, an index-2 DAE requires two differentiations, etc. After the index reduction, the governing equations can be written as a set of first-order ODEs.

B. Neural Differential Equations

A Neural Ordinary Differential Equation (NODE) approximates the flow map of a dynamical system with a neural network architecture. Consider a dynamical system with states $x \in \mathbb{R}^{n_x}$. A NODE approximates the temporal dynamics of x according to the ODE:

$$\frac{dx}{dt} = f(x; \theta), \quad (2)$$

where the parametric flow $f: \mathbb{R}^{n_x} \rightarrow \mathbb{R}^{n_x}$ maps the states to their time derivatives with tunable parameters θ . The solution to Eq. (2) is the initial value problem:

$$x^{(t+\Delta t)} = x^{(t)} + \int_t^{t+\Delta t} f(x; \theta) dt, \quad (3)$$

where the superscript contained in parentheses denotes indexing by time. This integration is performed with a standard numerical ODE solver, which we denote as:

$$x^{(t+\Delta t)} = \text{ODESolve}(f, x^{(t)}; \theta), \quad (4)$$

where the limits of temporal integration are understood to be $[t, t + \Delta t]$. In general, the NODE concept extends f to any differentiable mapping by implementing Eq. (4) in a differentiable manner [17]. This is achieved through either (i) backpropagating residuals through the elementary functions of the explicit time-stepping integrator (reverse-mode automatic differentiation) [26], [4], (ii) an adjoint sensitivity definition and solution [7], or (iii) forward-mode automatic differentiation [27].

III. PROBLEM FORMULATION

A fundamental assumption of a NODE model (2) is that a direct relationship exists between each system state and its temporal derivative. This is a reasonable assumption for many cases, but poses challenges for partially-observed systems [28] and application to DAEs. Index reduction is a reliable technique for recasting a DAE into a set of ODEs for standard numerical integration [29], but this is incompatible with the problem when the DAE governing equations are unknown or incomplete, leading to an unknown system of ODEs and required state augmentations.

To address this limitation, we aim to solve the following parameter estimation problem for neural DAEs (NDAE):

$$\min_{\Theta} \int_{t_0}^{t_N} \left(\|x - \hat{x}\|_2^2 + \|y - \hat{y}\|_2^2 \right) \quad (5a)$$

$$\text{s.t.} \quad \frac{dx}{dt} = f(x, y, u; \Theta), \quad (5b)$$

$$0 = g(x, y, u; \Theta), \quad (5c)$$

$$x(t_0) = x_0, \quad y(t_0) = y_0, \quad (5d)$$

Where \hat{x}, \hat{y} represent reference state variables generated by the unknown DAE system (1). The objective of the problem (5a) is to train the parameters Θ such that the reference state trajectories in the time interval $[t_0, t_N]$ are closely approximated by the NDAE model given via Eq. (5b) and Eq. (5d), respectively.

Assumptions 1: Lets consider the unknown DAE system (1) with f and g being continuously differentiable functions in a neighborhood of the point (x_0, y_0, u_0) . Suppose the following conditions hold:

- 1) (Regularity) The Jacobian matrix $\frac{\partial g}{\partial y}$ is nonsingular at (x_0, y_0, u_0) , i.e., $\det\left(\frac{\partial g}{\partial y}(x_0, y_0, u_0)\right) \neq 0$.
- 2) (Consistency) The initial values satisfy the algebraic constraint, i.e., $g(x_0, y_0, u_0) = 0$.

Theorem 3.1 (Picard-Lindelöf for index-1 DAEs [30]):

Under the above assumptions, there exists a unique, continuously differentiable solution $(x^{(t)}, y^{(t)})$ defined on an interval $[t_0, t_0 + \Delta t)$, for some $\Delta t > 0$, such that the DAE system is satisfied and $(x^{(t_0)}, y^{(t_0)}) = (x_0, y_0)$. Furthermore, the algebraic constraint can be locally solved for y as a function of x and u , thereby reducing DAEs into a system of ODEs $\frac{\partial x}{\partial t} = f(x, h(x, u), u)$ to which the classical Picard-Lindelöf Theorem 3.2 applies.

Theorem 3.2 (Classical Picard-Lindelöf for ODEs [31]):

Let $f : D \subseteq \mathbb{R}^{n_x} \times \mathbb{R}^{n_u} \rightarrow \mathbb{R}^{n_x}$ be a function that is continuous in both arguments and Lipschitz continuous with respect to the state x , uniformly in t , on an open set D containing the point (t_0, x_0) . Then there exists an interval $I = [t_0 - \epsilon, t_0 + \epsilon] \subset \mathbb{R}$, for some $\epsilon > 0$, and a unique continuously differentiable function $x : I \rightarrow \mathbb{R}^{n_x}$ such that

$$\frac{\partial x(t)}{\partial t} = f(x(t), u(t)), \quad x(t_0) = y_0,$$

for all $t \in I$. In other words, the ODE initial value problem has a unique local solution.

IV. METHOD

In this paper, we propose an efficient operator splitting (OS) numerical integration scheme for the neural DAE parameter estimation problem given by Eq. (5a). Specifically, we utilize the above Picard-Lindelöf Theorem 3.1 to derive a novel operator splitting-based numerical integration method for data-driven modeling of index-1 DAEs.

A. Operator Splitting Methods

Our methodology is inspired by operator splitting methods (OS) for evolving complex multiphysics problems. In OS, also called fractional step methods, the evolution of a system is split into simpler, independent sub-tasks. The underlying ODE is then solved explicitly as the sequential solution of these sub-tasks, albeit at a decreased level of accuracy (i.e., splitting error [32]). There are several well-established techniques for decomposing the solution of an ODE into sub-tasks. The simplest scheme, Lie-Trotter operator splitting [5], assumes a differential operator can be decomposed into two sub-tasks. For the ODE of Eq. (2), assume f can be decomposed into operators A and B such that:

$$\frac{dx}{dt} = A(x) + B(x), \quad (6)$$

for the interval $t \in [t, t + \Delta t]$. The Lie-Trotter splitting scheme defines the sub-tasks as:

$$\hat{x}^{(t+\Delta t)} = \text{ODESolve}\left(A(x), x^{(t)}\right), \quad (7)$$

$$x^{(t+\Delta t)} = \text{ODESolve}\left(B(x), \hat{x}^{(t+\Delta t)}\right). \quad (8)$$

The first sub-task solves the ODE defined by the operator $A(x)$ on the time interval $[t, t + \Delta t]$. The second sub-task solves the ODE defined by the operator $B(x)$ on the same time interval, but with the initial conditions defined by the solution of the first sub-task. Many variations of this scheme exist for different applications and orders of accuracy. For example, Strang splitting [33] is a second-order scheme that uses half-steps (i.e., steps of $\frac{\Delta t}{2}$) in the above scheme.

B. Operator Splitting for Differential Algebraic Equations

Now consider the DAE system of Eq. (1). Similar to the approach of a Lie-Trotter splitting scheme, we split the evolution of a system's differential and algebraic states into sequential sub-tasks. The first sub-task updates the algebraic states using a trainable deep neural network (DNN). The second sub-task takes as input the updated algebraic states and performs a single-step integration. These two sequential sub-tasks define one complete forward pass; all system states are updated exactly once. More formally, consider a differentiable ODE layer, denoted as ODESolve . Using the operator splitting method as our solution technique for Eq. (1), we formulate a time stepper for Neural DAE as:

$$y^{(t+\Delta t)} = h\left(x^{(t)}, y^{(t)}, u^{(t)}; \theta_h\right) \quad (9a)$$

$$x^{(t+\Delta t)} = \text{ODESolve}\left(f, \{x^{(t)}, y^{(t+\Delta t)}, u^{(t)}\}; \theta_f\right), \quad (9b)$$

where $h : \mathbb{R}^{n_x} \times \mathbb{R}^{n_y} \times \mathbb{R}^{n_u} \rightarrow \mathbb{R}^{n_y}$ pairs with g as an explicit algebra solver or trainable neural surrogate thereof and the temporal integration bounds are assumed to be $[t, t + \Delta t]$. We denote this complete set of operations as DAESolve , with one complete time step captured as:

$$\{x^{(t+\Delta t)}, y^{(t+\Delta t)}\} = \text{DAESolve}\left(f, h, \{x^{(t)}, y^{(t)}, u^{(t)}\}; \Theta\right), \quad (10)$$

where $\Theta = \{\theta_h, \theta_f\}$ is the set of all model parameters.

Note that in this formulation, the updates to the algebraic and differential states are sequential; that is, the ODESolve step is dependent upon the update to the algebraic states. The sub-tasks do not commute. This is an essential assumption that enables explicit updates for both algebraic states and differential states. Figure 1 depicts the handling of differential and algebraic states through the proposed OS-based NDAE integration scheme. The module generates an internal state $y^{(t+\Delta t)}$ that is processed by the subsequent ODESolve as an exogenous input, similar to the notion of Neural Controlled Differential Equations [34].

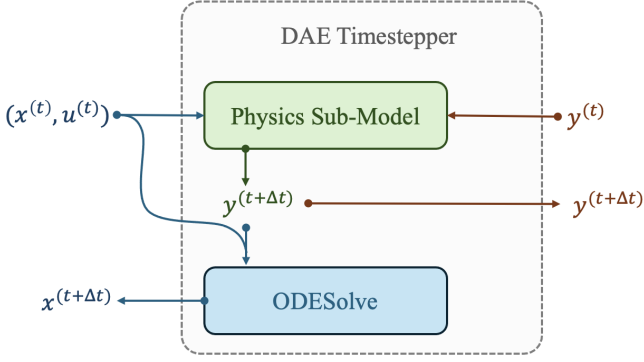


Fig. 1: Schematic of the proposed operator splitting-based DAE Timestepper.

C. Loss Function and Optimization Algorithm

In this paper, solving the algebraic update sub-task is accomplished by formulating a PINN-style penalty loss [6] in which known constraints are used to ‘penalize’ the discrepancy between constraint satisfaction and predicted states. These penalties are assessed in a multi-term loss function:

$$\mathcal{L}(\Theta) = \lambda_1 \mathcal{L}_{\text{residual}}(X, \hat{X}; \Theta) + \lambda_2 \mathcal{L}_{\text{constraints}}(X, \hat{X}; \Theta), \quad (11)$$

where $\mathcal{L}_{\text{residual}}(X, \hat{X}; \Theta) = \sum_{t=0}^N (\|x_t - \hat{x}_t\|_2^2 + \|y_t - \hat{y}_t\|_2^2)$ is a measure of the residual between the model’s differential and algebraic states $X = \{(x^{(0)}, y^{(0)}), \dots, (x^{(N)}, y^{(N)})\}$, and the training dataset $\hat{X} = \{(\hat{x}^{(0)}, \hat{y}^{(0)}), \dots, (\hat{x}^{(N)}, \hat{y}^{(N)})\}$, where N defines the length of a finite-horizon rollout. The second term $\mathcal{L}_{\text{constraints}}(X, \hat{X}; \Theta) = \sum_{t=0}^N \|g(x_t, y_t, u_t)\|_2^2$ is penalizing the constraint violations. The λ ’s represent weightings for balancing the multi-objective loss function.

We optimize model parameters Θ with an off-the-shelf stochastic gradient-based optimizer [35] to solve $\Theta^* = \text{argmin}_{\Theta} \mathcal{L}(\Theta)$. For this work, we choose minimal architectures for ease of implementation and exposition, as outlined in Alg. 1. We use a first-order explicit timestepper for the ODE integration and use a DNN as a neural surrogate of an algebra solver. However, the proposed OS-based NDAE scheme is more generic than that and allows the combination of higher-order ODE solvers with iterative algebraic solvers such as Newton’s method.

V. NUMERICAL CASE STUDIES

All experiments were performed using the NeuroMANCER Scientific Machine Learning (SciML) package [36] built on top of PyTorch [37]. The open-source implementation of the presented method and associated numerical examples are available at GitHub². Each presented model was trained using an Intel I9-9980 CPU laptop with a wall-clock training time on the order of 5 minutes.

²<https://github.com/pnml/NeuralDAEs>

Algorithm 1: Operator splitting-based DAE training

Data: $\hat{X} = \{(\hat{x}^{(0)}, \hat{y}^{(0)}), \dots, (\hat{x}^{(N)}, \hat{y}^{(N)})\}$: time series dataset with spacing Δt

Parameters: $\Theta = \{\theta_f, \theta_h\}$: trainable parameters for mappings f and h ;
gradient step-size hyperparameter η ;
loss function error tolerance ϵ

```

/* Pick appropriate integrator */
1 Function ODESolve ( $f, \{x, y, u\}$ ):
2    $x^* \leftarrow x + \Delta t \times f(x, y, u; \theta_f)$ 
3   return  $x^*$ 

/* Operator splitting via Eq. (9) */
4 Function DAESolve ( $f, h, \{x, y, u\}$ ):
5    $y^* \leftarrow h(x, y, u; \theta_h)$ 
6    $x^* \leftarrow \text{ODESolve}(f, \{x, y^*, u\}; \theta_f)$ 
7   return ( $x^*, y^*$ )

/* Training loop */
8 while  $\mathcal{L}(\Theta) > \epsilon$  do
   /* Forward pass */
9    $X \leftarrow \{(\hat{x}^{(0)}, \hat{y}^{(0)})\}$ 
10  for  $k \in 1, \dots, N$  do
11     $X \leftarrow \text{Concat}(X,$ 
12     $\quad \text{DAESolve}(f, h, \{x^{(k-1)}, y^{(k-1)}, u^{(k-1)}\})$ 
13     $)$ 
   /* Evaluate loss via Eq. (11) */
14    $\mathcal{L}(\Theta) \leftarrow \text{Criterion}(X, \hat{X})$ 
15   if  $\mathcal{L}(\Theta) \leq \epsilon$  then
16     break;
17   else
18     /* Backward pass */
19      $\nabla \mathcal{L}(\Theta) \leftarrow \frac{\partial \mathcal{L}(\Theta)}{\partial \Theta}$ 
20     /* Update model parameters */
21      $\Theta \leftarrow \Theta - \eta \nabla \mathcal{L}(\Theta)$ 

```

A. Tank-Manifold Property Inference

1) *Problem Description:* A manifold is a physical realization of a conservation relationship that manifests as an algebraic constraint in a DAE. Figure 2 depicts a pair of tanks fed by a manifold. A pseudo-infinite reservoir supplies the pump. At the manifold, the inflow is exactly equal to the sum of the outflows; that is, $y_{\text{in}} = y_1 + y_2$, where y represents volumetric flow rates and the subscripts 1 and 2 denote the two exit streams of the manifold. In this example, the two tanks have different area-height profiles but have a common datum such that the column heights are identical. As a fluid is pumped into the two tanks, the flow rates in the two streams varies to ensure (i) the conservation relationship of the manifold and (ii) that each of the tanks have identical pressure head, i.e. $x_1 = x_2$, where x is the height of the fluid in the respective tank. The full DAE that describes the evolution of this system is given as:

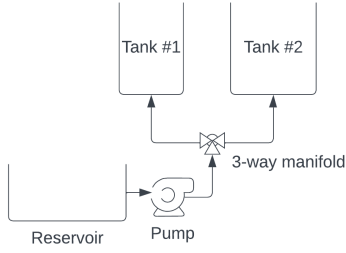


Fig. 2: Tank-manifold-pump schematic. A reservoir supplies fluid to a pump-manifold system. The tanks have different area-height profiles but a common datum. Conservation is enforced at the manifold.

$$\begin{aligned} \frac{dx_1}{dt} &= \frac{y_1}{\phi_1(x_1)} \\ \frac{dx_2}{dt} &= \frac{y_2}{\phi_2(x_2)} \end{aligned} \quad (12)$$

$$0 = y_{\text{in}} - y_1 - y_2 \quad 0 = x_1 - x_2,$$

where ϕ_1 and ϕ_2 denote the area-height profiles for the two tanks. The solution of Eq. (12) can be obtained with many off-the-shelf standard scientific computing packages. For this study, the area-height profiles are set to $\phi_1(x) = 3.0$ and $\phi_2(x) = \sqrt{x} + 0.1$ respectively. The goal of the learning task is to recover $\phi_2(x)$ given observations of tank heights x and pump volumetric flow rates y . Note that if the task were to recover both $\phi_1(x)$ and $\phi_2(x)$ simultaneously, the problem would be ill-posed in the sense that there does not exist a unique set of tank profiles that recovers the behavior seen in observations.

2) *Model Construction*: In the system described by Eq. (12), the differential states are column heights x_1 and x_2 and the algebraic states are the volumetric flows y_1 and y_2 . The input flow is treated as an exogenous control input, i.e., $u = y_{\text{in}}$. We aim to approximate the area-height profile of Tank #1 as well as construct a surrogate for the behavior of the manifold such that (i) fluid is conserved and (ii) the fluid column height constraint is satisfied. There are two neural networks that we seek to train: $NN_1 : \mathbb{R}^1 \rightarrow \mathbb{R}^1$, an approximation of the sought area-height profile ϕ_1 , and $NN_2 : \mathbb{R}^4 \rightarrow (0, 1)$, the surrogate of the behavior of the manifold. Each is implemented as a feed-forward neural network with one hidden layer of 5 nodes with sigmoid activation functions. The output layer of NN_1 is linear while the output layer of NN_2 is sigmoidal, constraining the output to $(0, 1)$.

3) *Optimization Problem*: A time series dataset \hat{X} is constructed by simulation of the system given in Eq. (12) regularly sampled on the interval $t \in [0, 500]$ with $\Delta t = 1.0$ and with a constant inflow of $y_{\text{in}} = u = 0.5$. The optimization problem seeks the minimum of the differential state trajectory reconstruction loss and algebraic state

reconstruction loss when predicted by our DAESolve:

$$\begin{aligned} \min_{\theta_1, \theta_2} \quad & \lambda_1 \sum_{k=1}^N \|x^{(k)} - \hat{x}^{(k)}\|_2^2 + \lambda_2 \sum_{k=1}^N \|y^{(k)} - \hat{y}^{(k)}\|_2^2 \\ \text{s.t.} \quad & \{x^{(k+1)}, y^{(k+1)}\} \\ & = \text{DAESolve} \left(f, h, \{x^{(k)}, y^{(k)}, u^{(k)}\}; \{\theta_1, \theta_2\} \right), \end{aligned} \quad (13)$$

The functions f and h are defined as:

$$\begin{aligned} f : \quad & \begin{cases} \frac{y_1}{3} \\ \frac{y_2}{NN_1(x_2; \theta_1)}, \end{cases} \\ h : \quad & \begin{cases} u NN_2(x_1, x_2, y_1, y_2; \theta_2) \\ u (1 - NN_2(x_1, x_2, y_1, y_2; \theta_2)), \end{cases} \end{aligned} \quad (14)$$

Note that the mapping h defines a convex combination at the manifold: the outflows y_1 and y_2 will sum to u by construction. For all examples contained in this work, the optimizer is Adam [35] with a fixed learning rate of 0.001. Training is deemed ‘converged’ after 20,000 epochs or until an early stop is triggered after 20 epochs of increasing loss.

4) *Results*: The time series data for the tank heights and volumetric flows are given in Figs. 3(a) and 3(b) respectively. The trained model is able to accurately reproduce the time series data seen in training. Additionally, it is able to accurately learn the model of the unknown area-height profile of Tank #2. Figure 4(a) depicts the ground-truth area-height profile and the model’s reconstruction. Furthermore, to demonstrate the generalization, the trained model is tested on an unseen inlet mass flow rate; $u(t) = \frac{1}{2} + \frac{1}{4} \sin\left(\frac{t}{100}\right)$. The resulting time series of volumetric flows from the trained model rollout is compared with the ground-truth conditions in Fig. 4(b). Table-I gives the Mean Squared Error (MSE) of the trained neural DAE model.

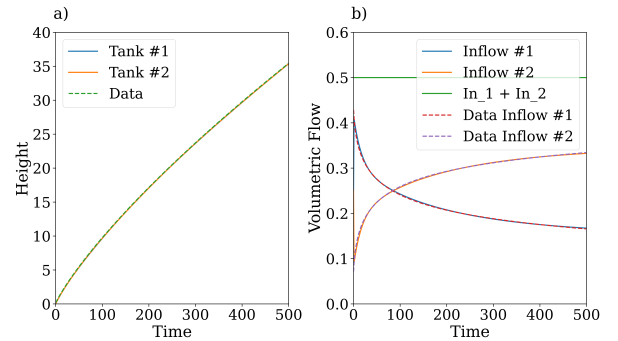


Fig. 3: (a) Tank heights. (b) Volumetric flow.

Extrapolation to a new flow condition demonstrates the ability to (i) endogenize the behaviors of the components in the network and their interaction physics and (ii) disambiguate between data trends and mechanistic relationships contained in the network.

B. Tank Network Modeling

1) *Problem Description*: Figure 5 expands upon the tank-manifold problem of Fig. 2 by adding additional tanks,

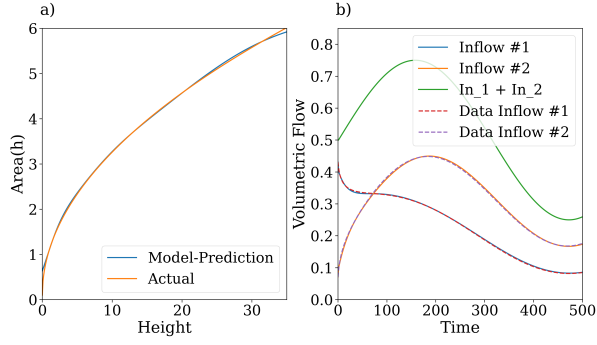


Fig. 4: Trained model (a) Area-height relationships (b) Volumetric flow time series.

TABLE I: Mean Square error for the differential state and algebraic states for the tanks-manifold-pump experiment.

Manifold	Mean Square Error (MSE)
Tanks Height	9e-03
Volumetric Flow	2e-02
Area-Height	6e-03
Unseen inlet mass-flow	1e-01

feedback mechanisms, and ‘closing the loop’ in the network flow. In this example, the pump flow rate depends on the fluid heights of Tank #1 and the reservoir. Tanks #1 and #2 have a height constraint (equivalent pressure head) and are fed by a common manifold. The outlets of tanks #1 and #3 depend on the square root of the fluid column height in the respective tanks. The full system is described by DAEs:

$$\begin{aligned}
 \frac{dx_1}{dt} &= \frac{1}{\phi_1(x_1)} (y_1 - y_3) \\
 \frac{dx_2}{dt} &= \frac{1}{\phi_2(x_2)} (y_2) \\
 \frac{dx_3}{dt} &= \frac{1}{\phi_3(x_3)} (y_3 - y_4) \\
 \frac{dx_4}{dt} &= \frac{1}{\phi_4(x_4)} (y_4 - y_0) \\
 0 &= y_0 - p(x_1, x_4) \quad 0 = y_0 - y_1 - y_2 \\
 0 &= y_3 - \alpha_1 \sqrt{x_1} \quad 0 = y_4 - \alpha_2 \sqrt{x_3} \\
 0 &= x_1 - x_2
 \end{aligned} \tag{15}$$

where x denotes the fluid column height for tanks #1 through #4 (the reservoir), p is a pump response function, y represents volumetric flows, and α describe the discharge coefficients of the tank outlets. The differential states are $x = \{x_1, x_2, x_3, x_4\} \in \mathbb{R}^4$ and the algebraic states are $y = \{y_0, y_1, y_2, y_3, y_4\} \in \mathbb{R}^5$. In this example, several characteristics make the dynamics more complex. First, the system is closed, as there is no material transfer into or out of the system. Second, there is the potential for backflow through the manifold from Tank #2. Lastly, the feedback mechanism from the tank level transducers to the pump controller is such that oscillations can occur.

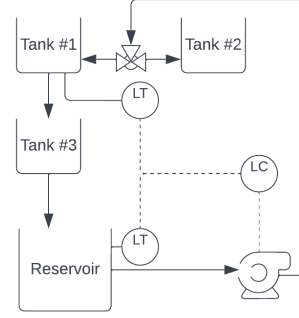


Fig. 5: Networked system defined by tanks, pipes, a manifold, and a pump. The system exhibits oscillatory dynamics for some parameter choices and sensing schemes.

2) *Optimization Problem:* The system given in Eq. (15) was simulated with the following specifications:

$$\begin{aligned}
 \phi_1(x_1) &= 2.0 & \phi_2(x_2) &= 1.0 \\
 \phi_3(x_3) &= 1.0 & \phi_4(x_4) &= 10.0 \\
 p(x_1, x_4) &= 0.1x_1x_4 & \alpha_1, \alpha_2 &= 0.1
 \end{aligned} \tag{16}$$

A single-trajectory dataset \hat{X} was constructed through sampling this simulation at $\Delta t = 0.1$ for $t \in [0, 20]$. The optimization problem definition is identical to that of Eq. (13). For this problem, it is reasonable to assume that the basic physics for a gravity-fed pipe network is known, which provides a starting point for constructing a model. However, discharge coefficients and quantifying feedback mechanisms are not as straightforward. Here, we attempt to approximate (i) the Level Controller (LC) dynamics for pump control with a neural network $NN_1 : \mathbb{R}^2 \rightarrow \mathbb{R}^1$, (ii) manifold dynamics with a second neural network $NN_2 : \mathbb{R}^2 \rightarrow \mathbb{R}^1$, and (iii) the discharge coefficients α_1 and α_2 . The mappings f and h are defined as:

$$\begin{aligned}
 f : & \begin{cases} \frac{y_1 - y_3}{\phi_1(x_1)} \\ \frac{y_2}{\phi_2(x_2)} \\ \frac{y_3 - y_4}{\phi_3(x_3)} \\ \frac{y_4 - y_0}{\phi_4(x_4)} \end{cases} \\
 h : & \begin{cases} NN_1(x_1, x_4; \theta_1) \\ y_0 NN_2(x_2, x_3; \theta_2) \\ y_0(1 - NN_2(x_2, x_3; \theta_2)) \\ \alpha_1 \sqrt{x_1} \\ \alpha_2 \sqrt{x_3} \end{cases}
 \end{aligned} \tag{17}$$

For this example, both NN_1 and NN_2 are simple multi-layer perceptrons, each with two hidden layers of size 30 and ReLU activations.

3) *Results:* Figure 6(a) details the time history of the four tank heights for both the ground truth data and the open-loop model rollout. At these process conditions, the pump delivers an oscillatory flow to the manifold, which our model is able to capture. Additionally, the tuned model can

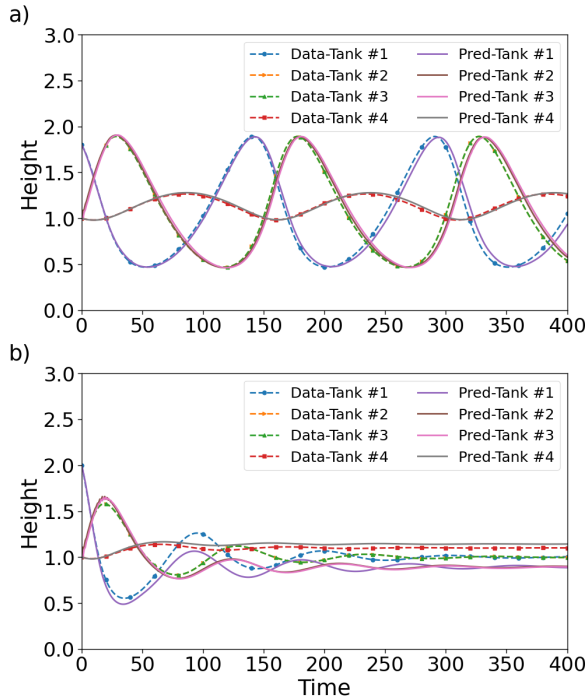


Fig. 6: Tank Network problem: (a) Ground truth data vs NDAE model prediction. (b) Extrapolation case: inferring behavior for unseen component parameters using NDAE.

infer the values for the discharge coefficients: for the case of zero noise, the recovered values are $\alpha_1 = 0.1027$ and $\alpha_2 = 0.1024$. To demonstrate generalizability, the trained model is deployed on an unseen area-height tank profile; for this, we redefine $\phi_1(x_1) = 1.0$. In doing so, the system's limit cycle is destroyed, and the true dynamics approach a steady state. Figure 6(b) demonstrates this extrapolation for the same time horizon. The reconstructed time series data matches the behavior of the unseen data: there exist damped oscillations that decay to a steady state value. Table II shows the MSE for the neural DAE models trained for the tank network problem. Noise tolerance is an important consideration in the evaluation of system identification tasks, especially in settings with nonlinearities and feedback mechanisms. For this example, we investigate noise tolerance by introducing Gaussian white noise. Figures 7(a) and 7(b) show similar training and extrapolation tasks for the Signal-to-Noise Ratio (SNR) of 20 dB. Despite the significant noise, the learned dynamics are faithful to the underlying physics, as demonstrated in the extrapolation task, and result in an MSE of $7e - 02$.

TABLE II: Mean Square error for the differential state and algebraic states for the tanks network experiment.

Trained Model Type	Tank-Network Experiment	Mean Square Error (MSE)
No Noise	Tanks Height	1e-02
	Unseen initial Data : Tanks Height	6e-02
20 dB Noise	Tanks Height	1.03
	Unseen initial Data : Tanks Height	7e-2

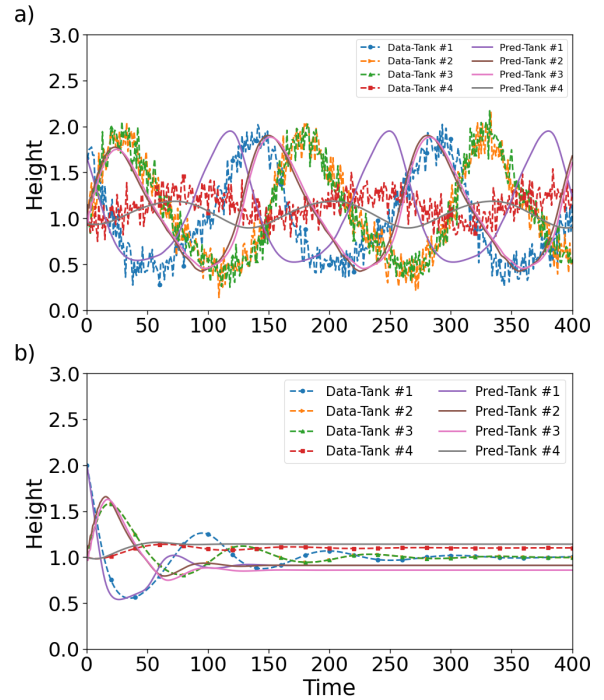


Fig. 7: Tank Network problem: (a) noisy data vs Neural-DAE model prediction. (b) Extrapolation case: inferring behavior for unseen component parameters using Neural-DAE.

VI. CONCLUSIONS AND FUTURE WORKS

This work presents a framework for the data-driven modeling of Differential Algebraic Equations (DAE). Specifically, we introduce a novel Operator Splitting (OS) integration method for Neural Differential Algebraic Equations (NDAE). Inspired by Lie-Trotter operator splitting, we achieve this by splitting the integration of system states into two sequential sub-tasks: first, updating algebraic states via a differentiable surrogate of an algebra solver, followed by a conventional temporal integration step for a system of Ordinary Differential Equations.

The effectiveness of the proposed method is demonstrated by (i) modeling networked dynamical systems with underlying constraints and conservation relationships and (ii) showing generalization to unseen process conditions or component variation. We demonstrate that the proposed OS-based NDAE method is robust to noise and possesses the extrapolation ability to (i) learn the behaviors of the DAE system components and their interaction physics and (ii) disambiguate between data trends and mechanistic relationships contained in the DAE system.

While the methods and example application problems were successful in this work, future research and development are needed in several areas. First, a central assumption of our method is that the underlying dynamics of the systems of interest are sufficiently smooth, i.e., not containing jump discontinuities or shocks, such that the underlying dynamics are non-stiff. As presented, our method leverages an explicit operator splitting method to decouple the evolution of the

differential and algebraic states. To increase the ability of the method to handle stiff dynamics or discontinuities, moving to an implicit integration scheme may be warranted. Second, further analysis is needed to investigate the interplay between the modeling task and the index of the underlying DAE (for example, higher-order DAEs that are characteristic of design or parameter optimization problems). Lastly, we have made no claims about computational scalability or partial observability, both of which are critical for modeling real-world complex systems with hundreds of degrees of freedom. We reserve these topics for future work.

ACKNOWLEDGMENTS

This research was supported by the U.S. Department of Energy through the Building Technologies Office under the Advancing Market-Ready Building Energy Management by Cost-Effective Differentiable Predictive Control projects. PNNL is a multi-program national laboratory operated for the U.S. Department of Energy (DOE) by Battelle Memorial Institute under Contract No. DE-AC05-76RL0-1830.

This research was also supported by the Ralph O'Connor Sustainable Energy Institute at Johns Hopkins University.

REFERENCES

- [1] P. Kunkel, *Differential-algebraic equations: analysis and numerical solution*, vol. 2. European Mathematical Society, 2006.
- [2] G. L. Mellor and T. Yamada, "Development of a turbulence closure model for geophysical fluid problems," *Reviews of Geophysics*, vol. 20, no. 4, pp. 851–875, 1982.
- [3] R. H. Bush, T. S. Chyczewski, K. Duraisamy, B. Eisfeld, C. L. Rumsey, and B. R. Smith, "Recommendations for future efforts in rans modeling and simulation," in *AIAA scitech forum*, 2019.
- [4] Y. Liu, J. N. Kutz, and S. L. Brunton, "Hierarchical deep learning of multiscale differential equation time-steppers," *Philosophical Transactions of the Royal Society A*, vol. 380, no. 2229, p. 20210200, 2022.
- [5] H. Holden, *Splitting methods for partial differential equations with rough solutions: Analysis and MATLAB programs*, vol. 11. European Mathematical Society, 2010.
- [6] G. E. Karniadakis, I. G. Kevrekidis, L. Lu, P. Perdikaris, S. Wang, and L. Yang, "Physics-informed machine learning," *Nature Reviews Physics*, vol. 3, no. 6, pp. 422–440, 2021.
- [7] R. T. Chen, Y. Rubanova, J. Bettencourt, and D. K. Duvenaud, "Neural ordinary differential equations," *Advances in neural information processing systems*, vol. 31, 2018.
- [8] C. Legaard, T. Schranz, G. Schweiger, J. Drgoña, B. Falay, C. Gomes, A. Iosifidis, M. Abkar, and P. Larsen, "Constructing neural network based models for simulating dynamical systems," *ACM Comput. Surv.*, vol. 55, feb 2023.
- [9] K.-i. Funahashi and Y. Nakamura, "Approximation of dynamical systems by continuous time recurrent neural networks," *Neural networks*, vol. 6, no. 6, pp. 801–806, 1993.
- [10] E. Skomski, S. Vasisht, C. Wight, A. Tuor, J. Drgoña, and D. Vrabie, "Constrained block nonlinear neural dynamical models," in *2021 American Control Conference (ACC)*, pp. 3993–4000, 2021.
- [11] A. Chakrabarty, G. Wichern, and C. R. Laughman, "Meta-learning of neural state-space models using data from similar systems," *IFAC-PapersOnLine*, vol. 56, no. 2, pp. 1490–1495, 2023. 22nd IFAC World Congress.
- [12] S. L. Brunton, J. L. Proctor, and J. N. Kutz, "Discovering governing equations from data by sparse identification of nonlinear dynamical systems," *Proceedings of the national academy of sciences*, vol. 113, no. 15, pp. 3932–3937, 2016.
- [13] J. O'Leary, J. A. Paulson, and A. Mesbah, "Stochastic physics-informed neural ordinary differential equations," *Journal of Computational Physics*, vol. 468, p. 111466, 2022.
- [14] S. Kim, W. Ji, S. Deng, Y. Ma, and C. Rackauckas, "Stiff neural ordinary differential equations," *Chaos: An Interdisciplinary Journal of Nonlinear Science*, vol. 31, p. 093122, 09 2021.
- [15] J. O. Ramsay, G. Hooker, D. Campbell, and J. Cao, "Parameter estimation for differential equations: a generalized smoothing approach," *Journal of the Royal Statistical Society: Series B (Statistical Methodology)*, vol. 69, no. 5, pp. 741–796, 2007.
- [16] T. X. Nghiem, J. Drgoña, C. Jones, Z. Nagy, R. Schwan, B. Dey, A. Chakrabarty, S. Di Cairano, J. A. Paulson, A. Carron, M. N. Zeilinger, W. Shaw Cortez, and D. L. Vrabie, "Physics-informed machine learning for modeling and control of dynamical systems," in *American Control Conference (ACC)*, pp. 3735–3750, 2023.
- [17] C. Rackauckas, Y. Ma, J. Martensen, C. Warner, K. Zubov, R. Supekar, D. Skinner, A. Ramadhan, and A. Edelman, "Universal differential equations for scientific machine learning," *arXiv preprint arXiv:2001.04385*, 2020.
- [18] J. Koch, Z. Chen, A. Tuor, J. Drgoña, and D. Vrabie, "Structural inference of networked dynamical systems with universal differential equations," *Chaos: An Interdisciplinary Journal of Nonlinear Science*, vol. 33, no. 2, p. 023103, 2023.
- [19] L. Petzold, R. Serban, S. Li, S. Raha, and Y. Cao, "Sensitivity analysis and design optimization of differential-algebraic equation systems," in *NATO Advanced Research Workshop on Computational Aspects of Nonlinear Structural Systems with Large Rigid Body Motion*, Pultusk, Poland, 2000.
- [20] Y. Cao, S. Li, L. Petzold, and R. Serban, "Adjoint sensitivity analysis for differential-algebraic equations: The adjoint dae system and its numerical solution," *SIAM journal on scientific computing*, vol. 24, no. 3, pp. 1076–1089, 2003.
- [21] J. B. Jorgensen, "Adjoint sensitivity results for predictive control, state-and parameter-estimation with nonlinear models," in *2007 European Control Conference (ECC)*, pp. 3649–3656, 2007.
- [22] C. Moya and G. Lin, "Dae-pinn: a physics-informed neural network model for simulating differential algebraic equations with application to power networks," *Neural Computing and Applications*, vol. 35, no. 5, pp. 3789–3804, 2023.
- [23] T. Xiao, Y. Chen, S. Huang, T. He, and H. Guan, "Feasibility study of neural ODE and DAE modules for power system dynamic component modeling," *IEEE Transactions on Power Systems*, 2022.
- [24] Y. Huang, C. Zou, Y. Li, and T. Wik, "Minn: Learning the dynamics of differential-algebraic equations and application to battery modeling," *arXiv preprint arXiv:2304.14422*, 2023.
- [25] Y. D. Zhong, B. Dey, and A. Chakraborty, "Extending lagrangian and hamiltonian neural networks with differentiable contact models," *Advances in Neural Information Processing Systems*, vol. 34, 2021.
- [26] S. H. Rudy, J. N. Kutz, and S. L. Brunton, "Deep learning of dynamics and signal-noise decomposition with time-stepping constraints," *Journal of Computational Physics*, vol. 396, pp. 483–506, 2019.
- [27] J. Revels, M. Lubin, and T. Papamarkou, "Forward-mode automatic differentiation in julia," *arXiv preprint arXiv:1607.07892*, 2016.
- [28] E. Dupont, A. Doucet, and Y. W. Teh, "Augmented neural odes," *Advances in neural information processing systems*, vol. 32, 2019.
- [29] S. E. Mattsson, H. Elmqvist, and M. Otter, "Physical system modeling with modelica," *Control engineering practice*, vol. 6, no. 4, pp. 501–510, 1998.
- [30] K. E. Brenan, S. L. Campbell, and L. R. Petzold, *Numerical Solution of Initial-Value Problems in Differential-Algebraic Equations*. Philadelphia, PA, USA: SIAM, 2 ed., 1996.
- [31] E. A. Coddington, *An Introduction to Ordinary Differential Equations*. Englewood Cliffs, NJ, USA: Prentice-Hall, 1961.
- [32] J. B. Perot, "An analysis of the fractional step method," *Journal of Computational Physics*, vol. 108, no. 1, pp. 51–58, 1993.
- [33] G. Strang, "On the construction and comparison of difference schemes," *SIAM journal on numerical analysis*, vol. 5, no. 3, 1968.
- [34] P. Kidger, J. Morrill, J. Foster, and T. Lyons, "Neural controlled differential equations for irregular time series," *Advances in Neural Information Processing Systems*, vol. 33, pp. 6696–6707, 2020.
- [35] D. P. Kingma and J. Ba, "Adam: A method for stochastic optimization," *arXiv preprint arXiv:1412.6980*, 2014.
- [36] J. Drgoña, A. Tuor, J. Koch, R. Birmival, M. Shapiro, and D. Vrabie, "NeuroMANNER: Neural Modules with Adaptive Nonlinear Constraints and Efficient Regularizations," 2023. <https://github.com/pnnl/neuromancer>.
- [37] A. Paszke, S. Gross, F. Massa, A. Lerer, J. Bradbury, G. Chanan, T. Killeen, Z. Lin, N. Gimelshein, L. Antiga, et al., "Pytorch: An imperative style, high-performance deep learning library," *Advances in neural information processing systems*, vol. 32, 2019.